

# **Searching for the Cosmic Dawn with the Hyperfine Structure Transition of Hydrogen**

---

**Michael W. Eastwood**

**Thesis Defense**

**September 3, 2018**

## Caltech

Gregg Hallinan  
Sandy Weinreb  
Larry D'Addario  
Stephen Bourke → Chalmers  
Jake Hartman → Google  
Harish Vedantham  
Jonathon Kocz  
Kate Clark  
Marin Anderson  
Ryan Monroe  
Devin Cody  
David Wang

## Harvard/SAO

Lincoln Greenhill  
Ben Barsdell → NVIDIA  
Danny Price → Swinburne  
Hugh Garsden  
Gianni Bernardi → SKA

## OVRO

David Woody  
James Lamb  
OVRO staff

## JPL

Joe Lazio

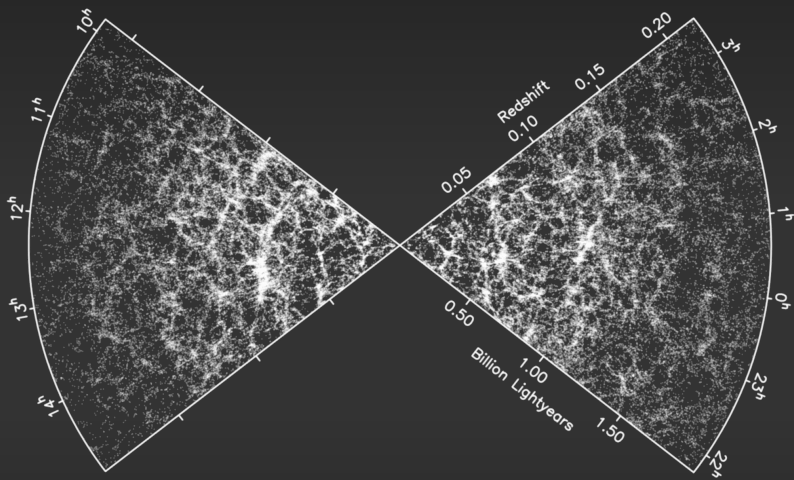
and the rest of the LWA team

# This Thesis

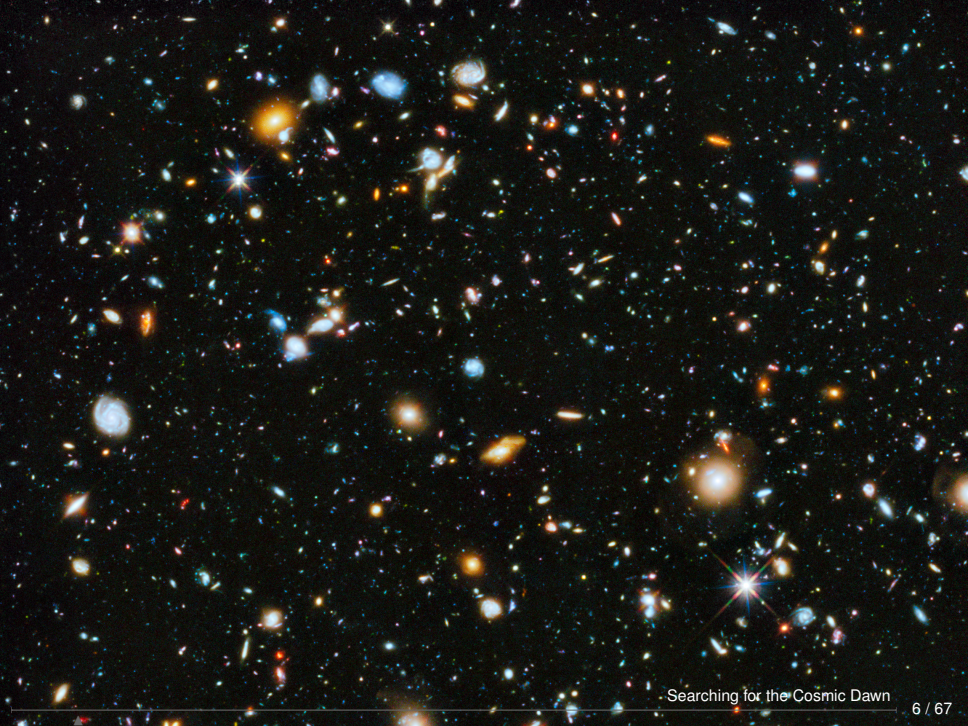
---

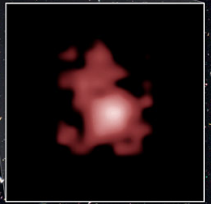
- I. Introduction to 21 cm Cosmology
- II. Commissioning the OVRO-LWA
- III. New Maps of the Sky at Meter Wavelengths
- IV. Upper Limits on the 21 cm Power Spectrum ( $z > 18$ )

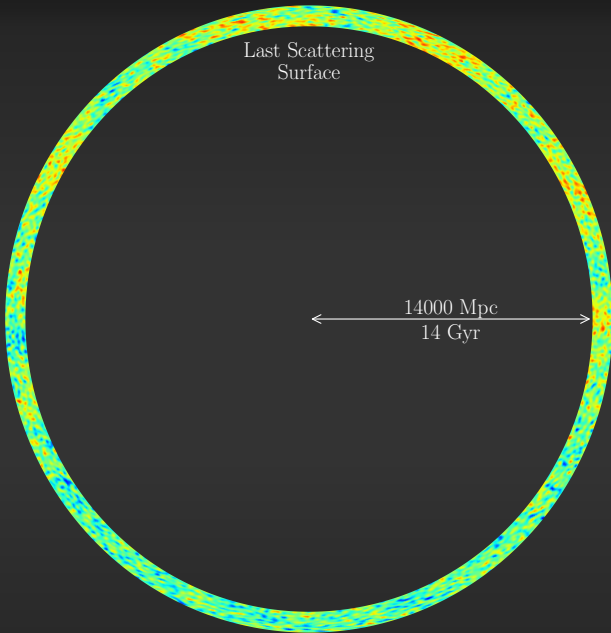
# I. Introduction to 21 cm Cosmology

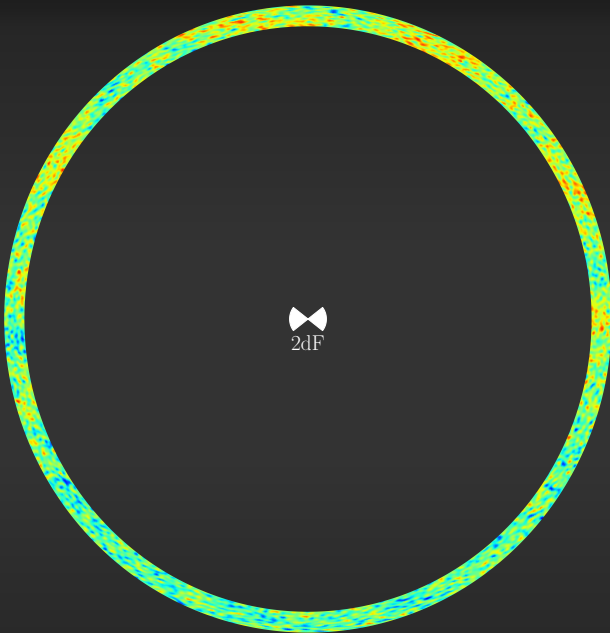


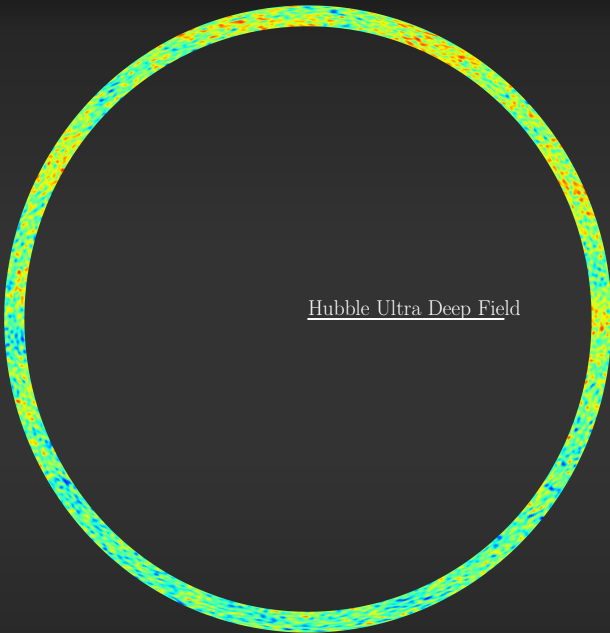
Colless et al. (2001)



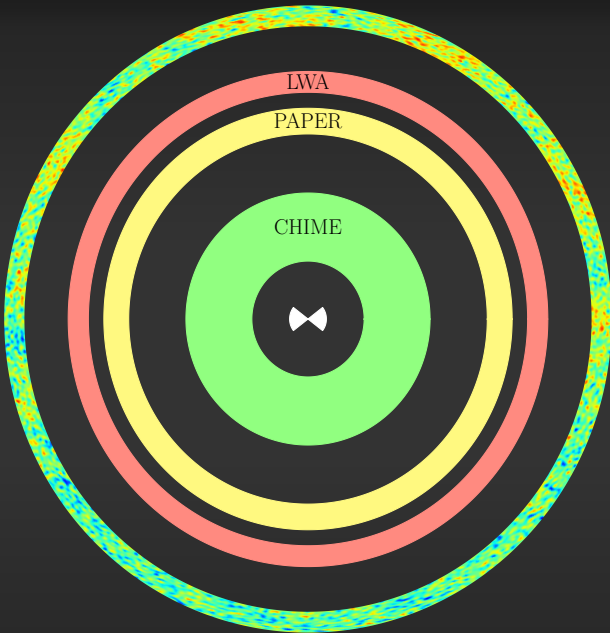


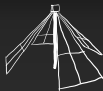




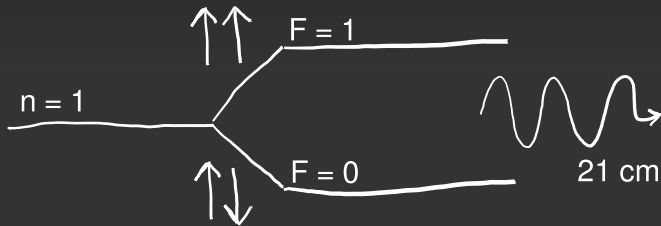


Hubble Ultra Deep Field

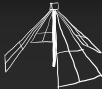




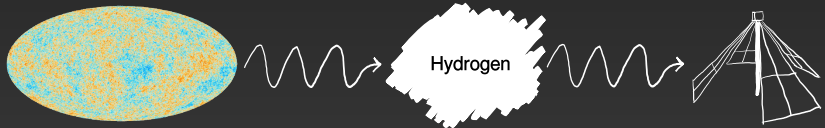
# Hyperfine Structure



- Magnetic dipole transition → very weak
- Optically thin tracer of HI
- Spin temperature  $\sim$  excitation state



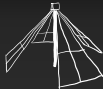
# Radiative Transfer



$$T_{21} \sim 27 \left[ \underbrace{x_{\text{HI}}(1 + \delta) \left( \frac{\Omega_b h}{0.0327} \right) \left( \frac{\Omega_m}{0.307} \right)^{-1/2} \left( \frac{1 + z}{10} \right)^{1/2}}_{\text{quantity of HI}} \times \underbrace{\left( \frac{T_{\text{spin}} - T_{\text{CMB}}(z)}{T_{\text{spin}}} \right)}_{\text{relative temperature}} \right] \text{ mK}$$

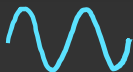
Pritchard &amp; Loeb (2012)

Searching for the Cosmic Dawn

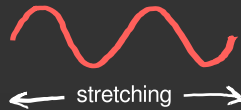


# Cooling

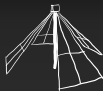
Radiation



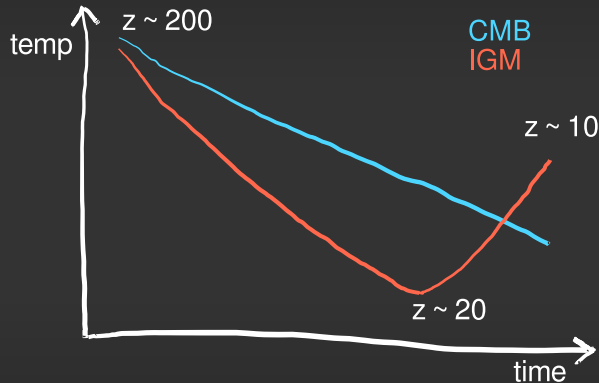
Matter

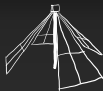


adiabatic  
expansion

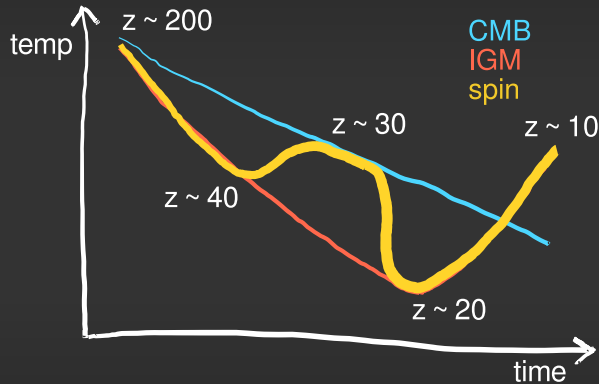


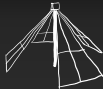
# Temperature History



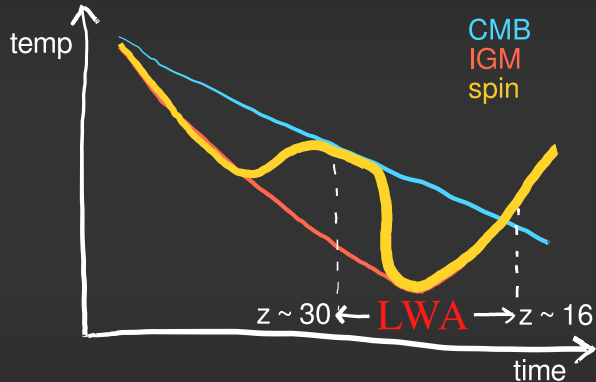


# Temperature History



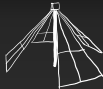


# Temperature History

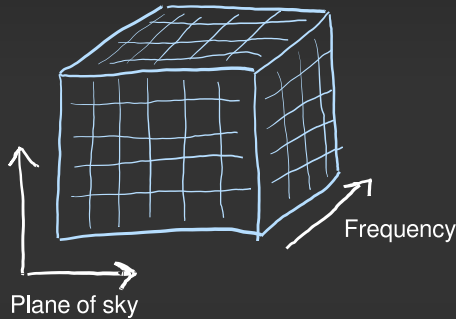




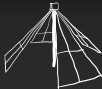
Alvarez et al. (2009)



# The 3D Spatial Power Spectrum



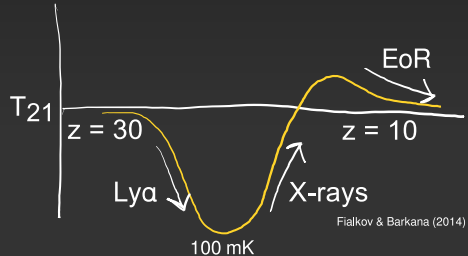
Fourier transform and square the brightness temperature in the cosmological cube.



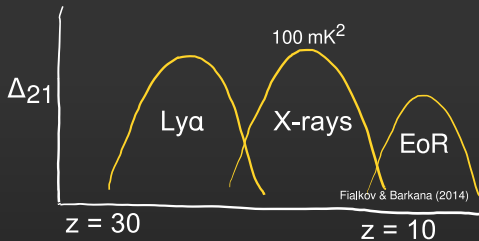
## I. Introduction

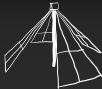
# The 21 cm Signal

"COBE"  
globally averaged  
brightness temperature



"WMAP"  
amplitude-squared of  
brightness temperature  
fluctuations





---

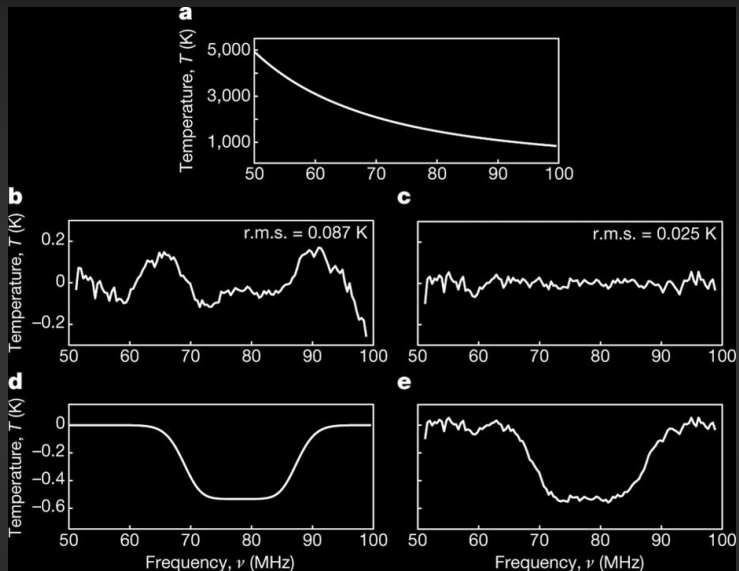
# Astrophysics from the Cosmic Dawn

Effects that influence the 21 cm signal:

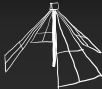
- Timing of early star formation
- Inhomogeneous star formation
- Relative motion of baryons relative to dark matter

(Tseliakhovich & Hirata 2010)

- Lyman-Werner feedback
  - (Fialkov et al. 2013)
- Flux and hardness of high-mass X-ray binaries
  - (Fialkov & Barkana 2014)



Bowman et al. (2018)



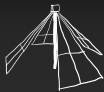
## New Ideas

- Baryon–dark matter interactions  
(Barkana 2018)
- New population of high-redshift radio sources  
(Ewall-Wice et al. 2018)
- $\Omega_b = \Omega_m$

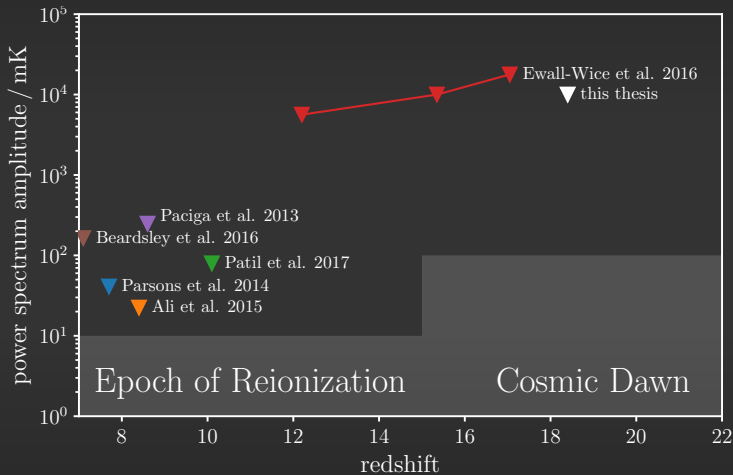
Generally, theoretical explanations of the Bowman et al. 2018 result predict an enhanced power spectrum amplitude ( $\sim 7\times$ ).

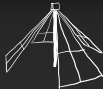
LWA GMRT LOFAR MWA PAPER





# Power Spectrum Upper Limits

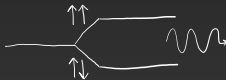




## I. Introduction

# Foregrounds in 21 cm Cosmology

Cosmological signal



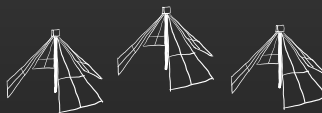
Extragalactic point sources



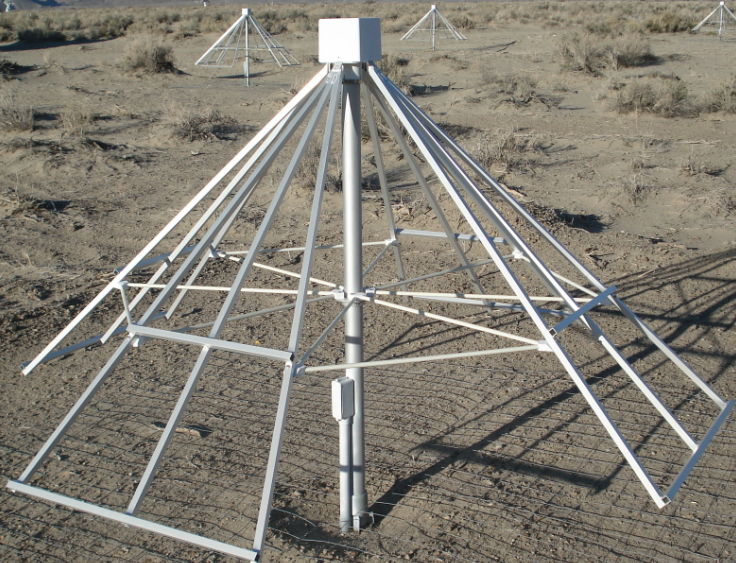
Galactic synchrotron emission



Ionosphere



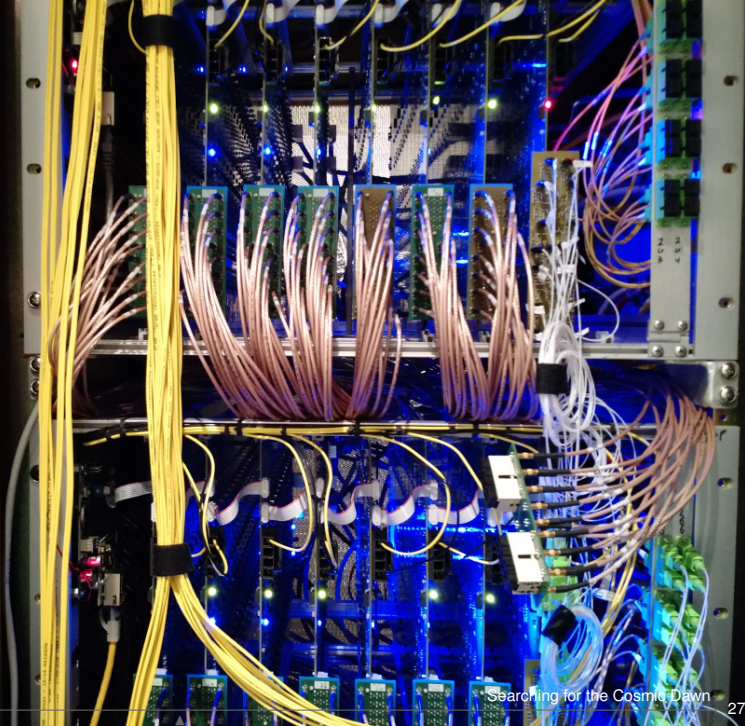
## II. Commissioning the OVRO-LWA





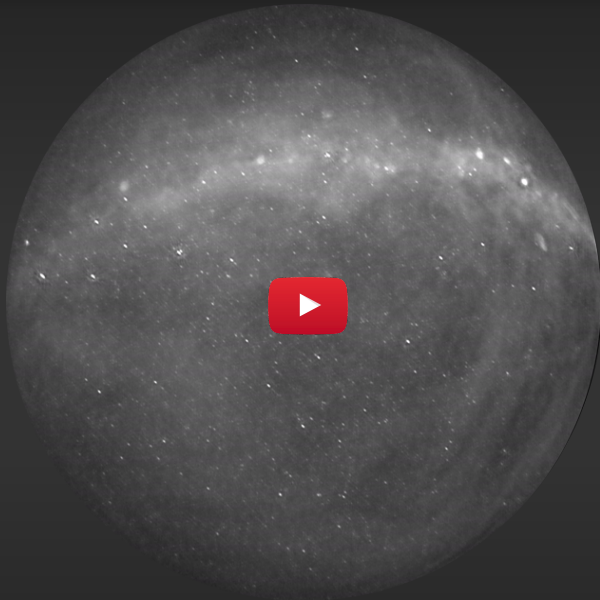










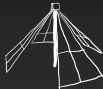




## II. The OVRO-LWA

# The OVRO-LWA

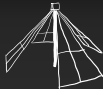
<b>Number of Antennas</b>	288 (256 correlated)
<b>Core Diameter</b>	200 m
<b>Maximum Baseline</b>	1.5 km
<b>Resolution</b>	10–20 arcmin
<b>Frequency Range</b>	27–85 MHz
<b>Frequency Resolution</b>	24 kHz
<b>Field of View</b>	Entire hemisphere
<b>Integration Time (this work)</b>	28 hr



---

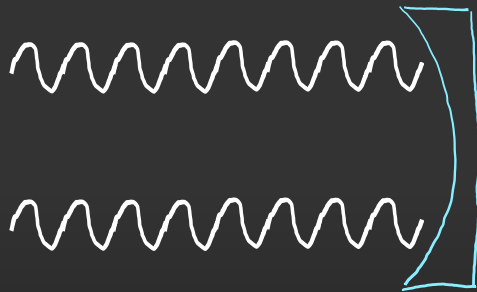
## Commissioning Challenges

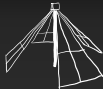
- Gain calibration
- Gain fluctuations
- Direction-dependent calibration
- Antenna positions
- Frequency labels
- RFI localization
- Common-mode RFI
- Primary beam mapping



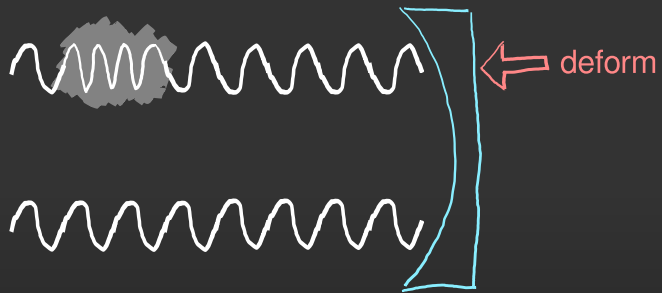
---

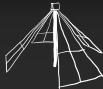
## Adaptive Optics



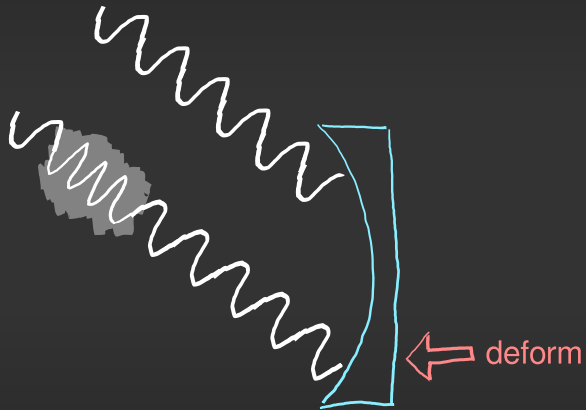


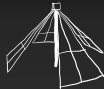
## Adaptive Optics





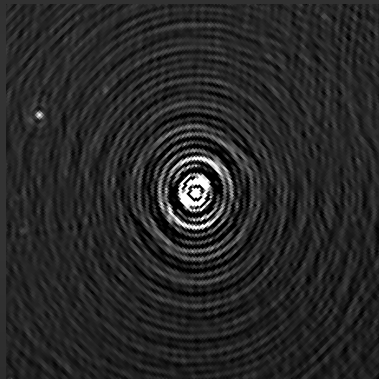
## Adaptive Optics

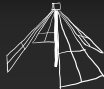




## Direction-Dependent Calibration

Image of Cas A prior to removal

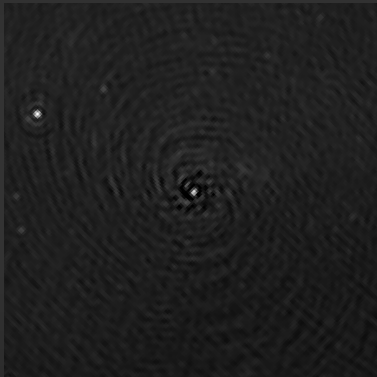


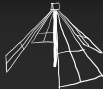


## II. The OVRO-LWA

# Direction-Dependent Calibration

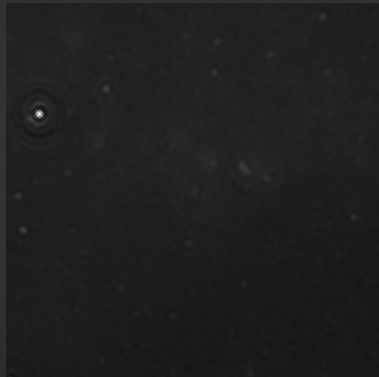
... after removing **without** direction dependent calibration





## Direction-Dependent Calibration

... after removing **with** direction dependent calibration



## The Cosmic Dawn

- First generation of stars
- Formation and feedback
- Heating of the IGM
- Early X-ray sources

## Transients

- Stellar flares
- Extrasolar planets
- SWIFT and LIGO follow-up
- See Anderson thesis

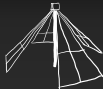
## Space Weather

- Solar flares
- Jovian flares

## Cosmic Rays

- Real-time detection
- See Monroe thesis

### III. New Maps of the Sky at Meter Wavelengths

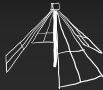


### III. VHF Sky Maps

## Imaging and Cleaning

$$\text{visibility} = \int (\text{sky brightness}) \times (\text{beam}) \times (\text{fringe pattern}) \, d\Omega$$

Shaw et al. (2014, 2015)



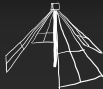
### III. VHF Sky Maps

## Imaging and Cleaning

$$\text{visibility} = \int (\text{sky brightness}) \times (\text{beam}) \times (\text{fringe pattern}) d\Omega$$

visibility  $\xrightarrow{\text{sidereal time Fourier transform}}$  m-mode

Shaw et al. (2014, 2015)



### III. VHF Sky Maps

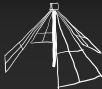
## Imaging and Cleaning

$$\text{visibility} = \int (\text{sky brightness}) \times (\text{beam}) \times (\text{fringe pattern}) d\Omega$$

visibility  $\xrightarrow{\text{sidereal time Fourier transform}}$  m-mode

$$\underbrace{\begin{pmatrix} \vdots \\ \text{m-modes} \\ \vdots \end{pmatrix}}_v = \underbrace{\begin{pmatrix} \ddots & & \\ & \text{transfer matrix} & \\ & & \ddots \end{pmatrix}}_B \underbrace{\begin{pmatrix} \vdots \\ a_{lm} \\ \vdots \end{pmatrix}}_a$$

Shaw et al. (2014, 2015)



### III. VHF Sky Maps

## Imaging and Cleaning

$$\text{visibility} = \int (\text{sky brightness}) \times (\text{beam}) \times (\text{fringe pattern}) d\Omega$$

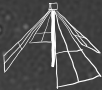
visibility  $\xrightarrow{\text{sidereal time Fourier transform}}$  m-mode

$$\underbrace{\begin{pmatrix} \vdots \\ \text{m-modes} \\ \vdots \end{pmatrix}}_v = \underbrace{\begin{pmatrix} \ddots & & \\ & \text{transfer matrix} & \\ & & \ddots \end{pmatrix}}_B \underbrace{\begin{pmatrix} \vdots \\ a_{lm} \\ \vdots \end{pmatrix}}_a$$

Shaw et al. (2014, 2015)

$$\hat{\mathbf{a}} = \operatorname{argmin} \left\{ \|v - B\mathbf{a}\|^2 + \varepsilon \|\mathbf{a}\|^2 \right\} = (B^* B + \varepsilon I)^{-1} B^* v$$

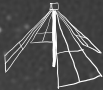
Eastwood et al. (2018)



### III. VHF Sky Maps

---

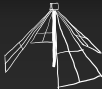
## Dirty Map



### III. VHF Sky Maps

---

## Clean Map



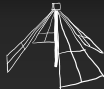
## Advantages and Disadvantages

### Advantages

- No gridding step
- No mosaicing step
- Exact treatment of widefield effects
- Optimal foreground filters

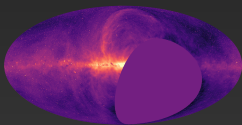
### Disadvantages

- Matrix equation is block diagonal, but still large!
- 500 GB/frequency channel (!)
- Rapid ionospheric changes break assumptions

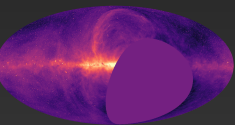


### III. VHF Sky Maps

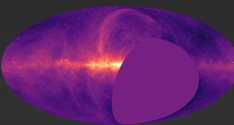
## Eight New Low-Frequency Sky Maps



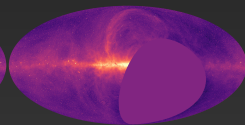
36.528 MHz



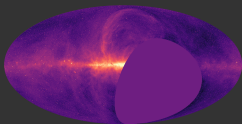
41.760 MHz



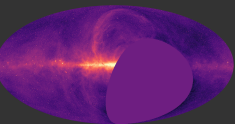
46.992 MHz



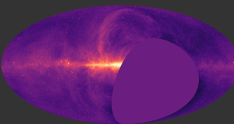
52.224 MHz



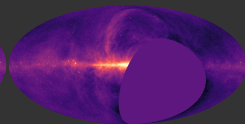
57.456 MHz



62.688 MHz



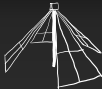
67.920 MHz



73.152 MHz

Eastwood et al. (2018)

[https://lambda.gsfc.nasa.gov/product/foreground/ovrolwa\\_radio\\_maps\\_info.cfm](https://lambda.gsfc.nasa.gov/product/foreground/ovrolwa_radio_maps_info.cfm)

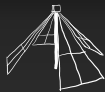


### III. VHF Sky Maps

## Map Properties

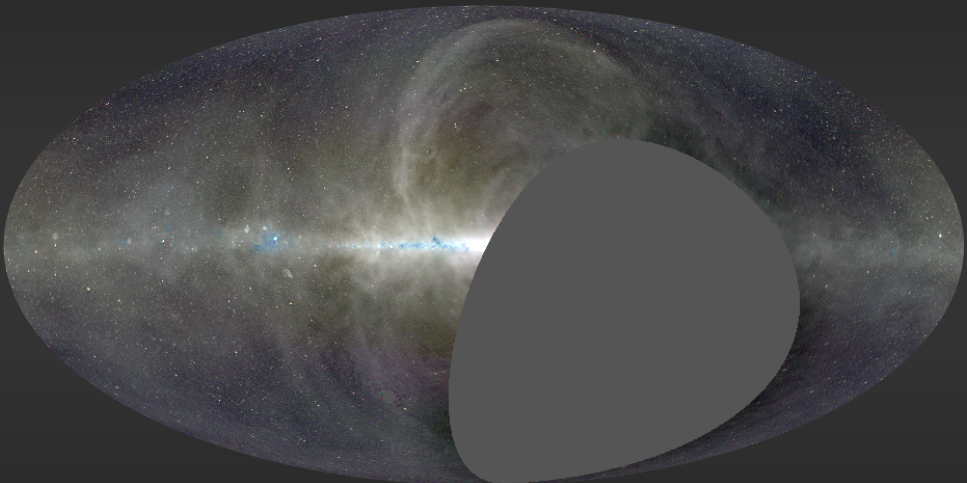
#	Frequency	Bandwidth	FWHM	Noise	
	MHz	kHz	arcmin	K	mJy/beam
1	36.528	24.	18.5	595.	799.
2	41.760	24.	17.2	541.	824.
3	46.992	24.	16.3	417.	717.
4	52.224	24.	15.6	418.	814.
5	57.456	24.	15.4	354.	819.
6	62.688	24.	15.3	309.	843.
7	67.920	24.	15.3	281.	894.
8	73.152	24.	15.7	154.	598.

Eastwood et al. (2018)

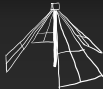


### III. VHF Sky Maps

## A Three Color Image

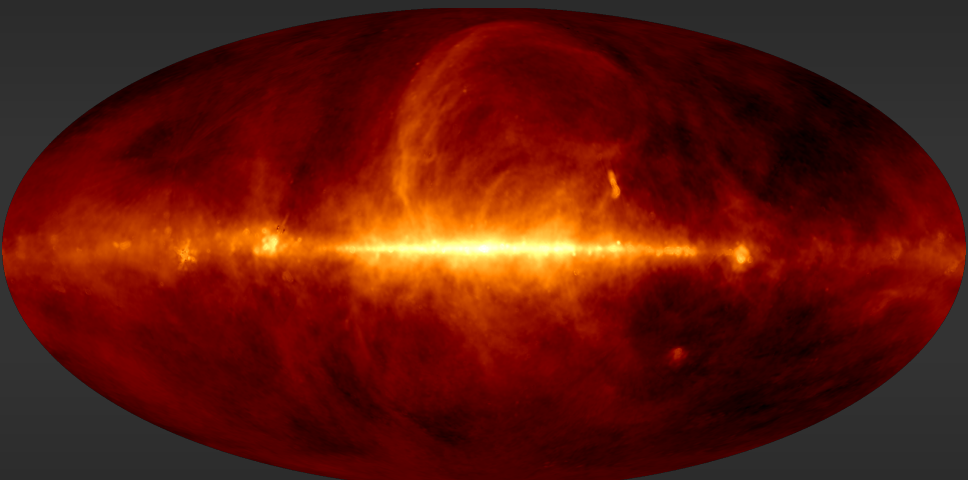


Eastwood et al. (2018)

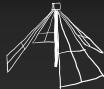


### III. VHF Sky Maps

## Comparison with Haslam 408 MHz

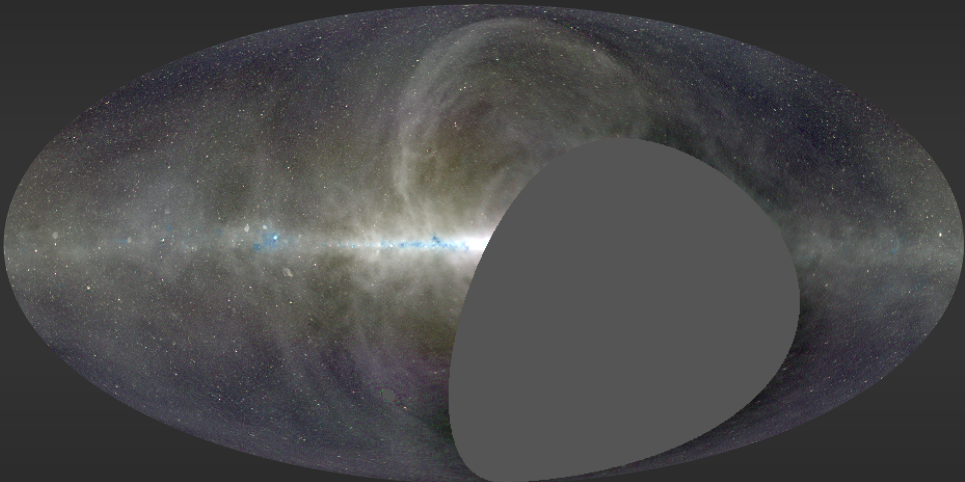


Haslam et al. (1981, 1982)

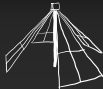


### III. VHF Sky Maps

## Comparison with Haslam 408 MHz

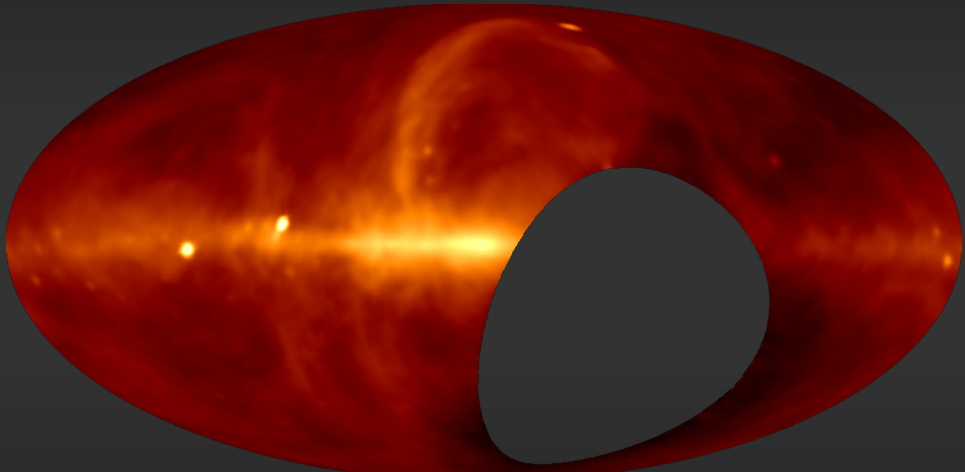


Eastwood et al. (2018)



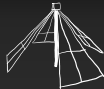
### III. VHF Sky Maps

## Comparison with LWA1 (35–80 MHz)



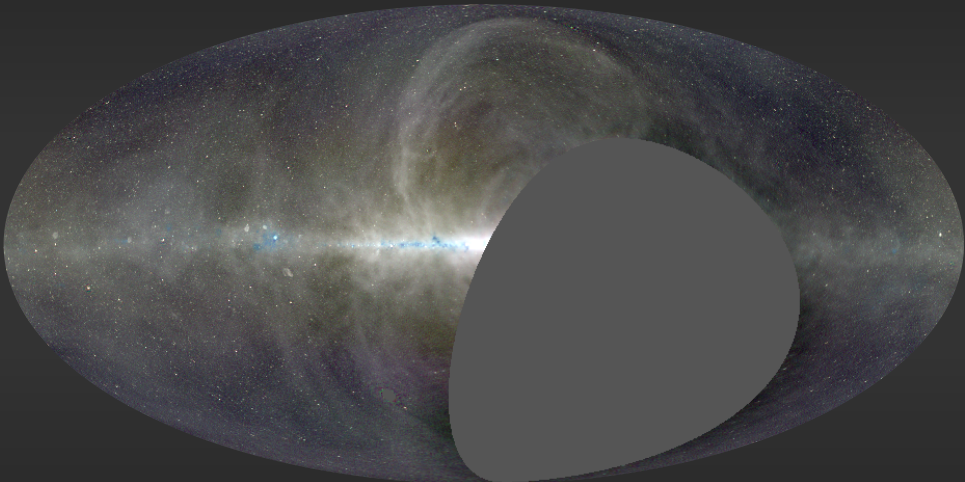
Dowell et al. (2017)

Searching for the Cosmic Dawn

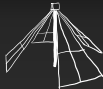


### III. VHF Sky Maps

## Comparison with LWA1 (35–80 MHz)

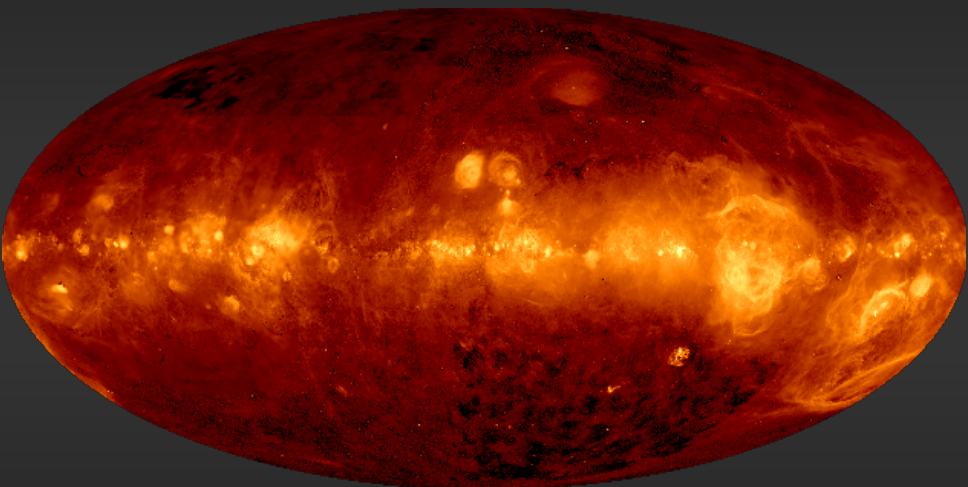


Eastwood et al. (2018)

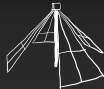


### III. VHF Sky Maps

## Comparison with Finkbeiner H $\alpha$

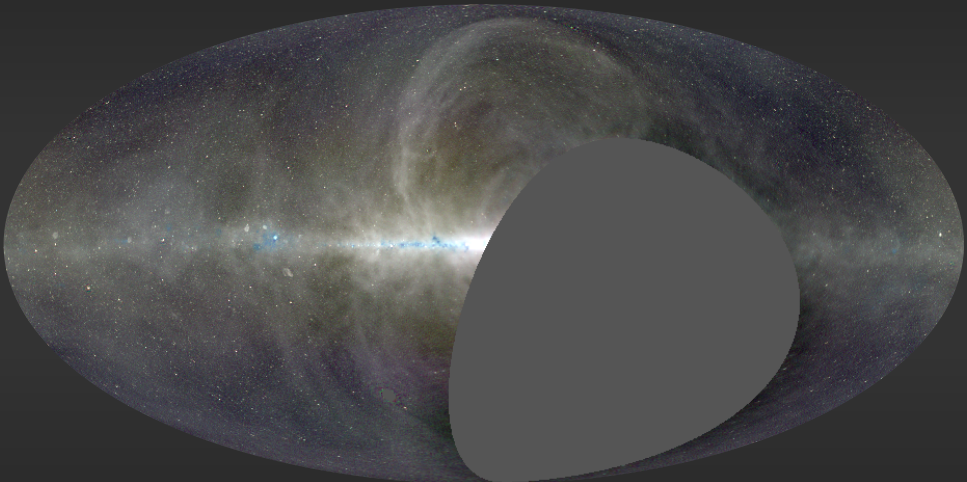


Finkbeiner et al. (2003)

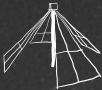


### III. VHF Sky Maps

## Comparison with Finkbeiner H $\alpha$



Eastwood et al. (2018)

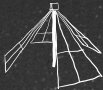


### III. VHF Sky Maps

---

## Higher Resolution, Higher Sensitivity

Eastwood et al. (2018)



### III. VHF Sky Maps

---

## Higher Resolution, Higher Sensitivity

Eastwood et al. (in prep.)

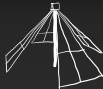


## Summary

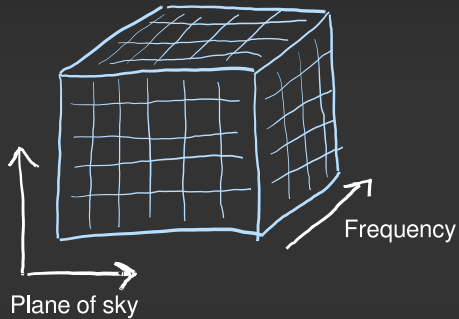
- Foreground maps are going to be extremely important for 21-cm cosmology experiments going forward.
- Creating high-fidelity foreground maps is also challenging.
- These maps are publicly available online.

[https://lambda.gsfc.nasa.gov/product/foreground/ovrolwa\\_radio\\_maps\\_info.cfm](https://lambda.gsfc.nasa.gov/product/foreground/ovrolwa_radio_maps_info.cfm)

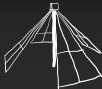
## IV. Upper Limits on the 21 cm Power Spectrum ( $z > 18$ )



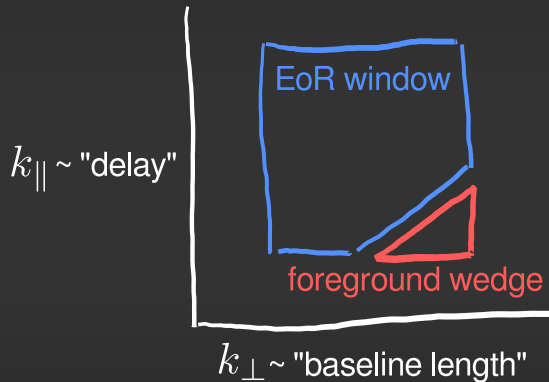
## The 3D Spatial Power Spectrum

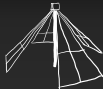


Fourier transform and square the brightness temperature in the cosmological cube.



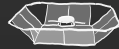
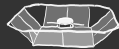
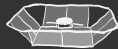
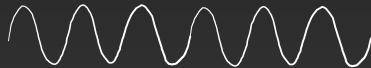
## The Foreground Wedge



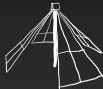


---

## The Foreground Wedge



$k_{\perp} \sim \text{"baseline length"}$



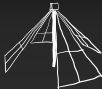
## The Foreground Wedge

### XF Correlator

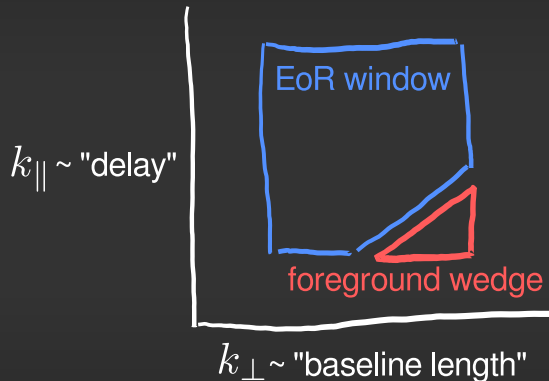
1. Cross-correlate voltages at series of time lags (“delays”)
2. Fourier transform to obtain frequency spectrum

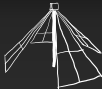
The Fourier transform along the line of sight undoes the correlator F-stage:

$$k_{\parallel} \sim \text{“delay”}$$



## The Foreground Wedge

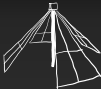




## Problems with the Foreground Wedge

- **Assumes** foreground emission is “smooth enough”
- **Does not** use any information about the angular structure of the foreground emission
- **Does not** use any information about the cosmological emission
- **Does not** account for wide-field effects

Thyagarajan et al. 2015



---

## Covariance Matrices

Key advantage of  $m$ -mode analysis: Full covariance matrices

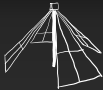
$$\langle \mathbf{v} \mathbf{v}^* \rangle = \mathbf{C} = \mathbf{C}_{21} + \mathbf{C}_{\text{fg}} + \mathbf{C}_{\text{noise}}$$

Typical size without  $m$ -mode analysis:

$$(N_{\text{baselines}} \times N_{\text{frequencies}} \times N_{\text{times}})^2 \times 128 \text{ bits} \sim 65 \text{ EB}$$

Typical size with  $m$ -mode analysis (per matrix block):

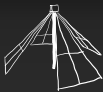
$$(l_{\max} \times N_{\text{frequencies}})^2 \times 128 \text{ bits} \sim 137 \text{ MB}$$



## The Noise Covariance

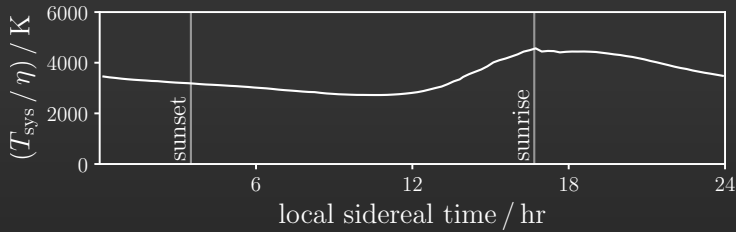
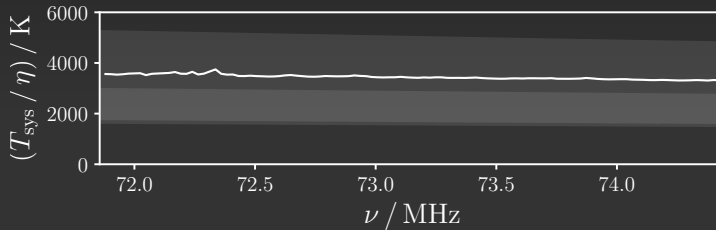
$$\langle \mathbf{v} \mathbf{v}^* \rangle = \mathbf{C} = \mathbf{C}_{21} + \mathbf{C}_{\text{fg}} + \boxed{\mathbf{C}_{\text{noise}}}$$

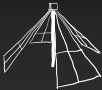
- Typically diagonal (although see Kulkarni 1989)
- Characterized by the system temperature  $T_{\text{sys}}$
- Measured from variance of visibilities after differencing
- Expect sky noise dominated with contribution from receiver



## IV. 21 cm Power Spectrum

# The Noise Covariance





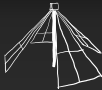
---

## The Foreground Covariance

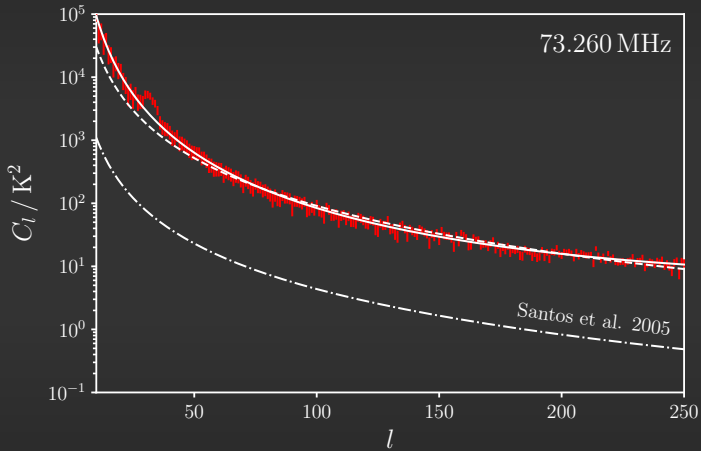
$$\langle \mathbf{v} \mathbf{v}^* \rangle = \mathbf{C} = \mathbf{C}_{21} + \boxed{\mathbf{C}_{\text{fg}}} + \mathbf{C}_{\text{noise}}$$

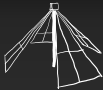
$$\left\langle a_{lm}(\nu) a_{l'm'}(\nu + \Delta\nu) \right\rangle = C_l(\nu, \Delta\nu) \delta_{ll'} \delta_{mm'}$$

- Dominated by the galactic synchrotron emission
- Contribution of point sources increases on small angular scales
- Measured  $C_l(\nu, 0)$  with an optimal quadratic estimator



## The Foreground Covariance





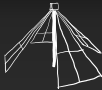
## The 21 cm Signal Covariance

$$\langle \mathbf{v} \mathbf{v}^* \rangle = \mathbf{C} = [\mathbf{C}_{21}] + \mathbf{C}_{\text{fg}} + \mathbf{C}_{\text{noise}}$$

$$P_{\text{model}}(k) = \frac{2\pi^2}{k^3} \min \left[ 40 \left( \frac{k}{0.03 \text{ Mpc}^{-1}} \right)^2, 400 \right] \text{ mK}^2$$

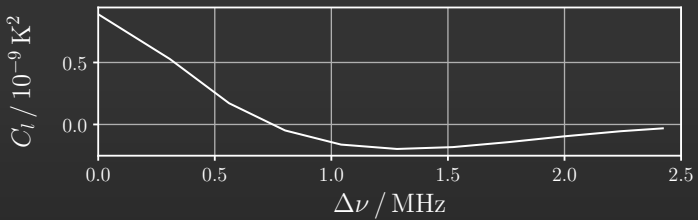
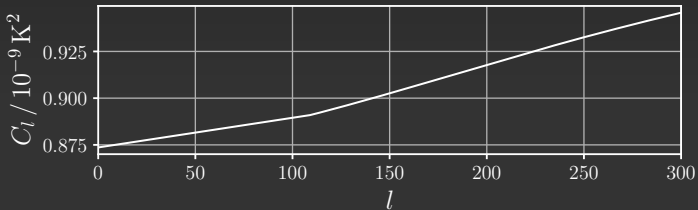
- Simple fiducial model (Fialkov et al. 2014)
- If EDGES detection is true, power spectrum amplitude reasonably expected to be 50 times brighter

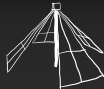
(Bowman et al. 2018, Barkana 2018)



## IV. 21 cm Power Spectrum

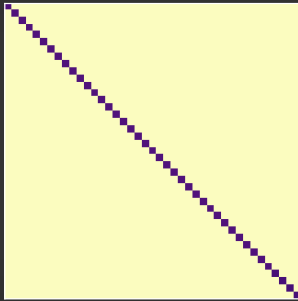
# The 21 cm Signal Covariance



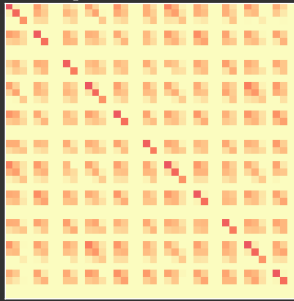


## The Karhunen–Loève Transform

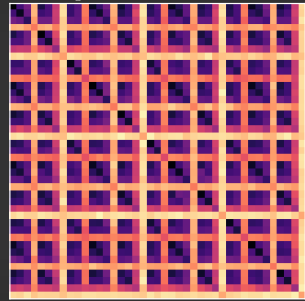
noise covariance matrix

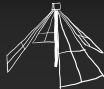


signal covariance matrix



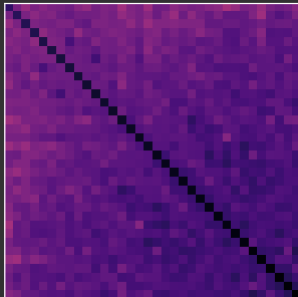
foreground covariance matrix



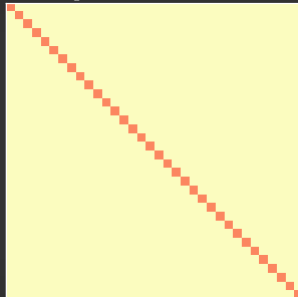


## The Karhunen–Loève Transform

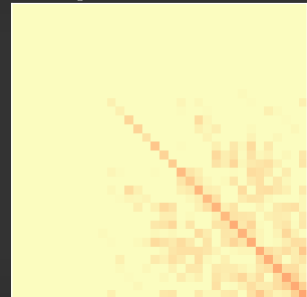
noise covariance matrix

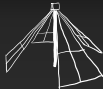


signal covariance matrix



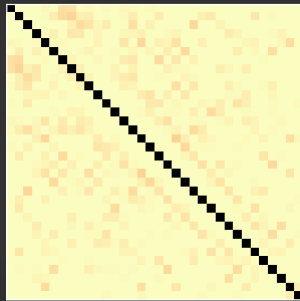
foreground covariance matrix



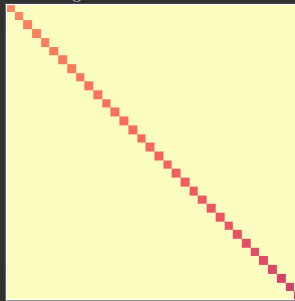


## The Karhunen–Loève Transform

noise covariance matrix

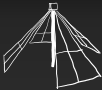


signal covariance matrix



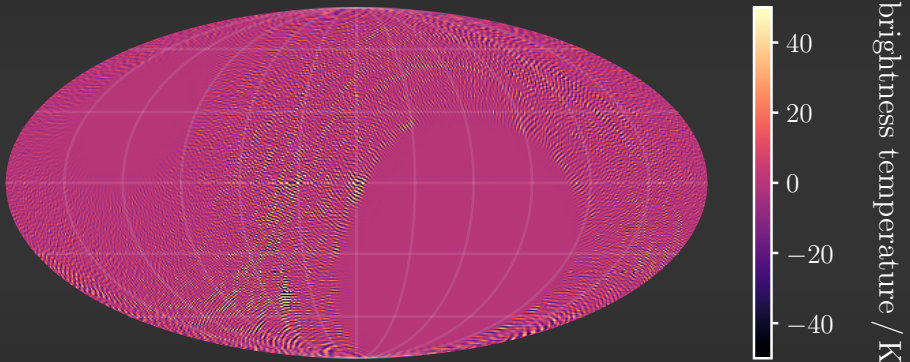
foreground covariance matrix

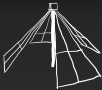




## IV. 21 cm Power Spectrum

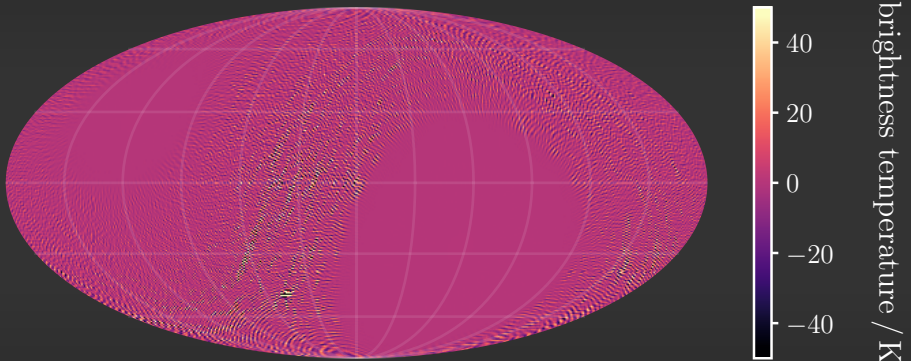
### Filtered Image

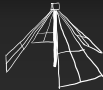




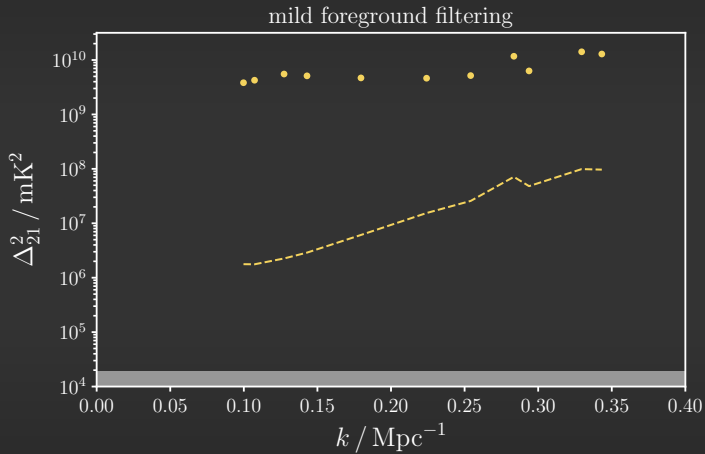
## IV. 21 cm Power Spectrum

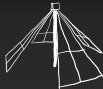
### Filtered Image



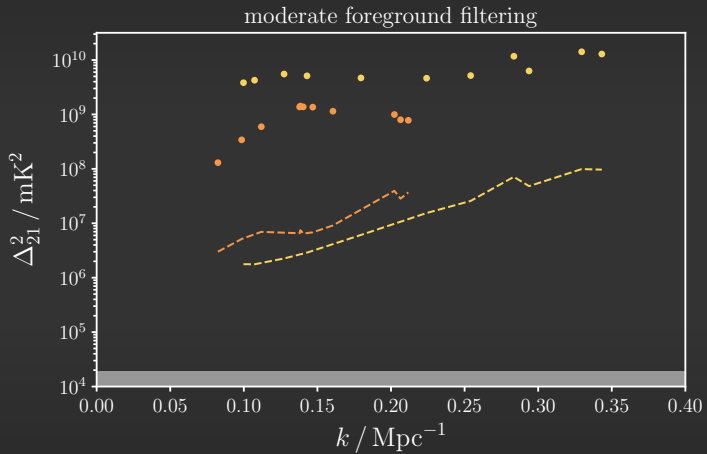


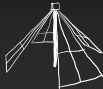
## Power Spectrum Estimate



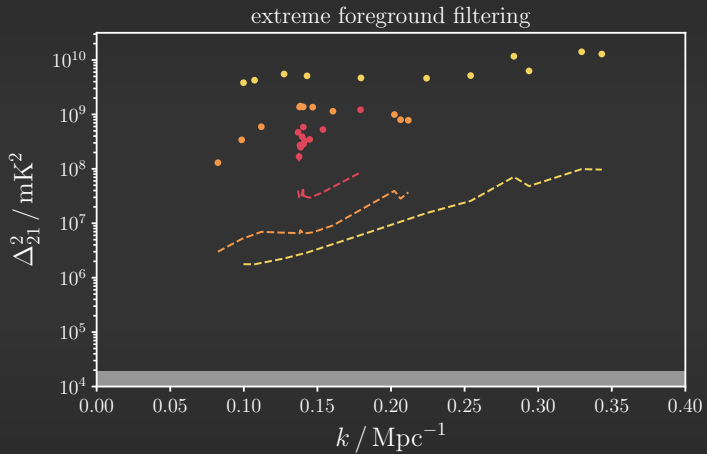


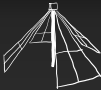
## Power Spectrum Estimate





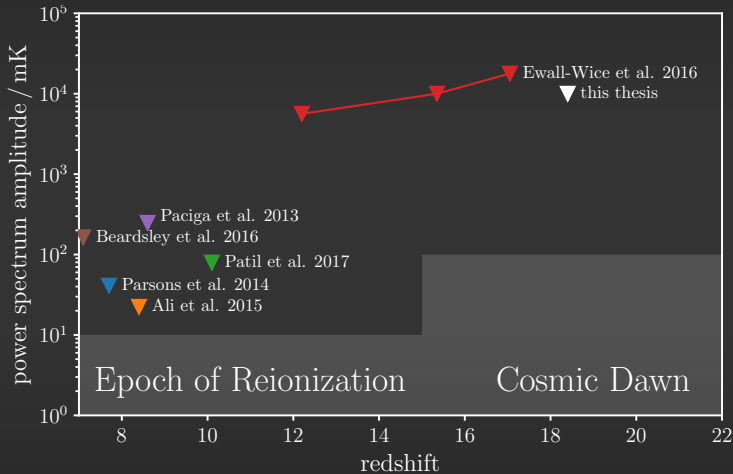
# Power Spectrum Estimate

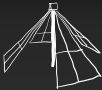




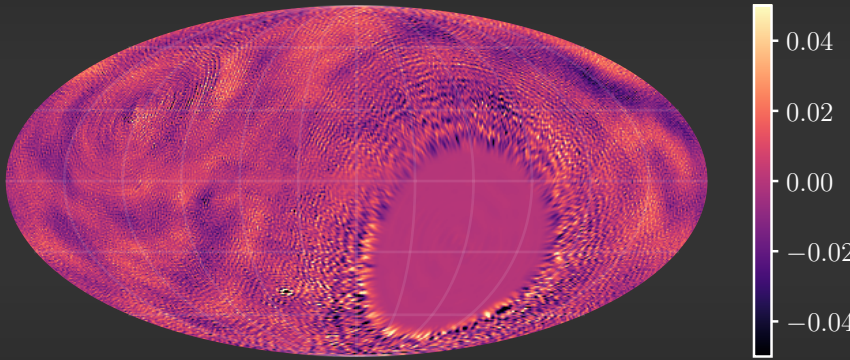
#### IV. 21 cm Power Spectrum

## Power Spectrum Limits

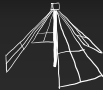




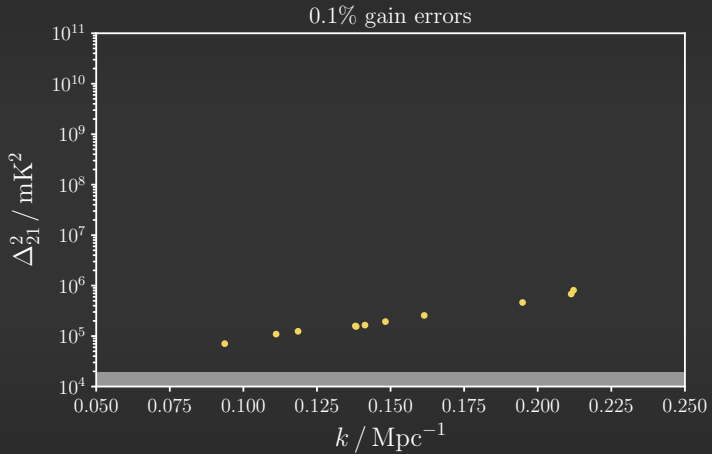
## Bandpass Errors

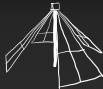


fractional difference

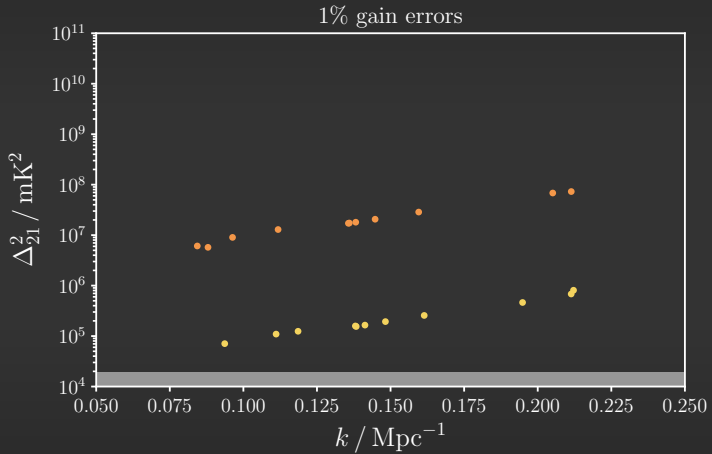


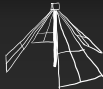
# Systematic Limitations



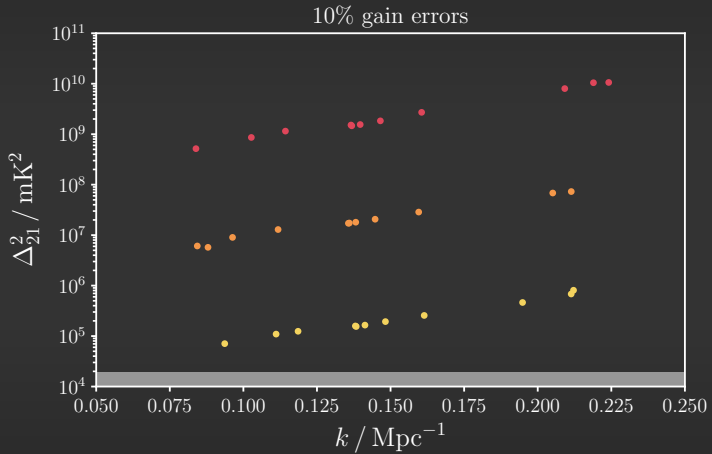


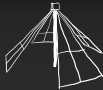
## Systematic Limitations



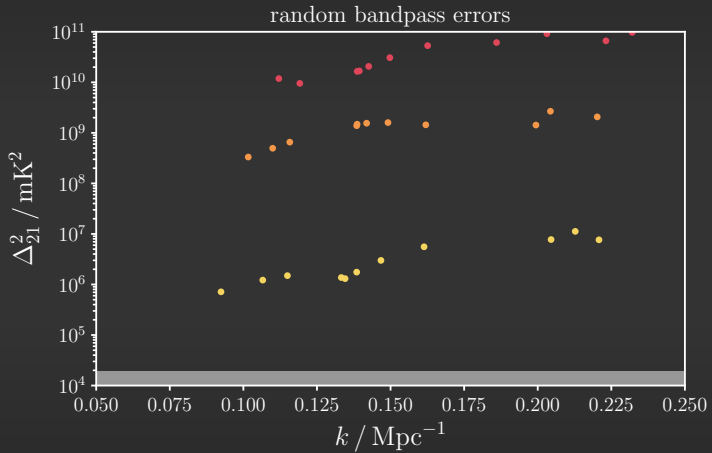


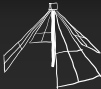
# Systematic Limitations





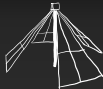
## Systematic Limitations





## Conclusions

- First measured upper limit of the 21 cm power spectrum at  $z > 18$
- Lowest upper limit  $\Delta_{21}^2 \lesssim (10^4 \text{ mK})^2$
- The double KL transform foreground filter is effective if gain errors  $< 0.1\%$  and bandpass errors  $< 0.01\%$
- Current upper limits from the OVRO-LWA are consistent with  $\sim 1\%$  errors in the bandpass

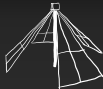


## Summary

# This Thesis

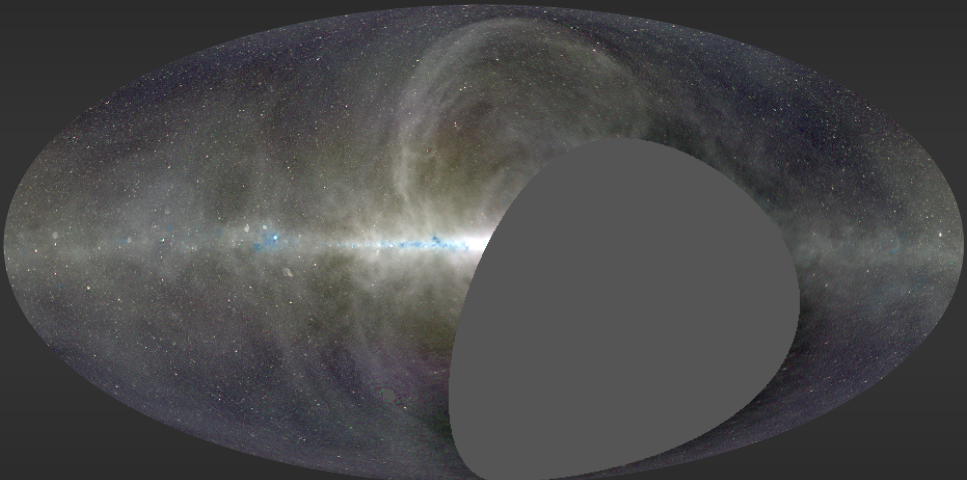
---

- I. Introduction to 21 cm Cosmology
- II. Commissioning the OVRO-LWA
- III. New Maps of the Sky at Meter Wavelengths
- IV. Upper Limits on the 21 cm Power Spectrum ( $z > 18$ )

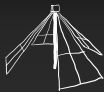


---

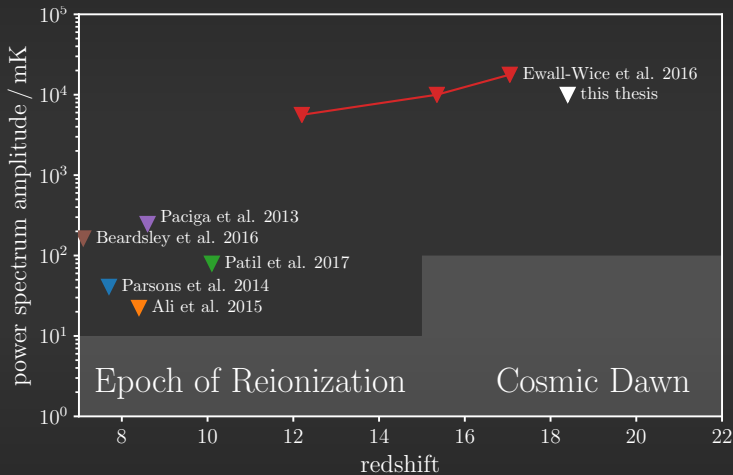
## A Three Color Image



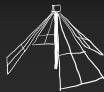
Eastwood et al. (2018)



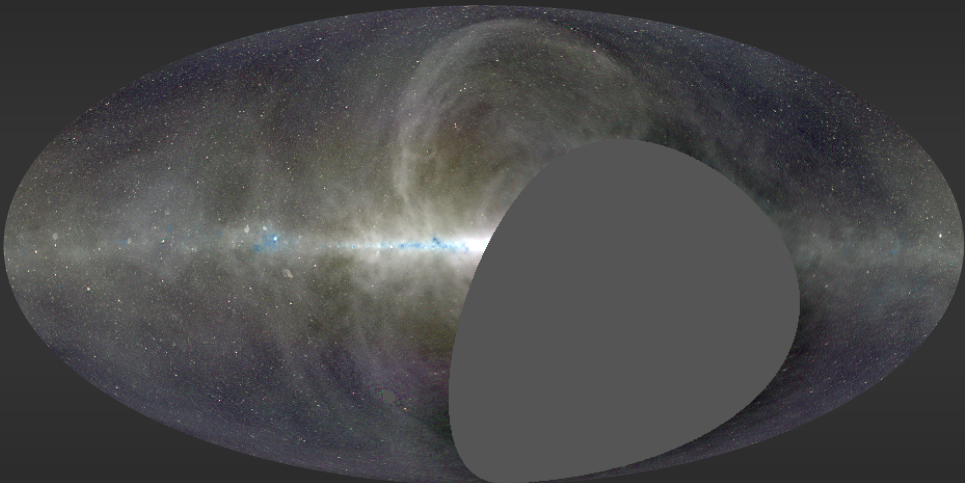
# Power Spectrum Limits



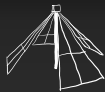
# Backup Slides



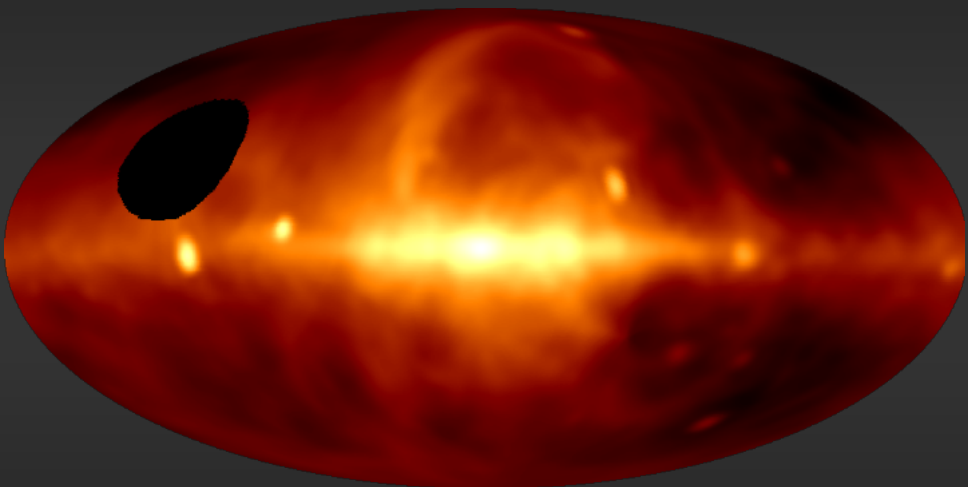
## Comparison with Guzmán 45 MHz



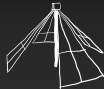
Eastwood et al. (2018)



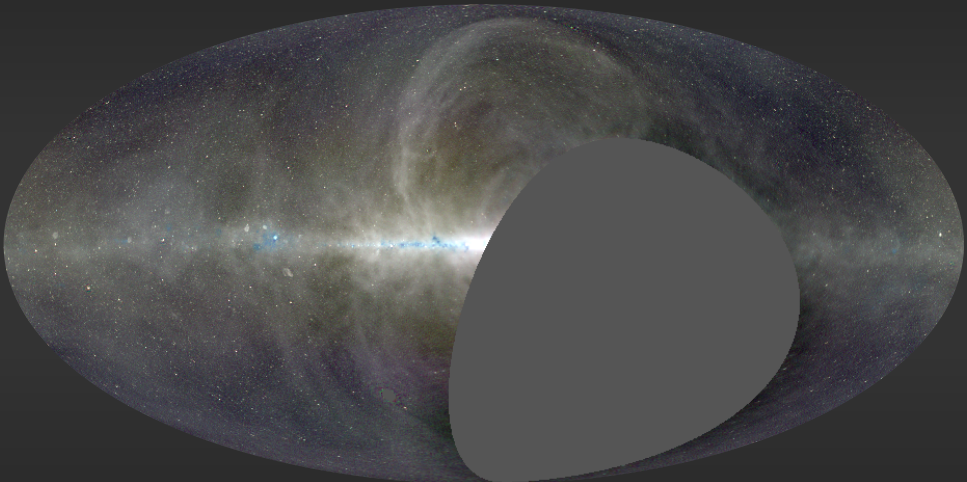
## Comparison with Guzmán 45 MHz



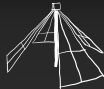
Guzmán et al. (2011)



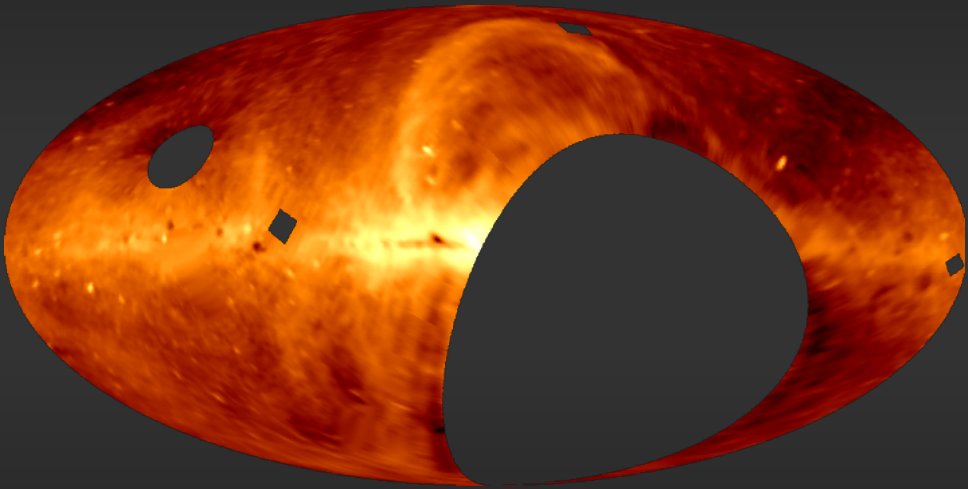
## Comparison with DRAO 22 MHz



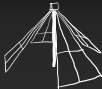
Eastwood et al. (2018)



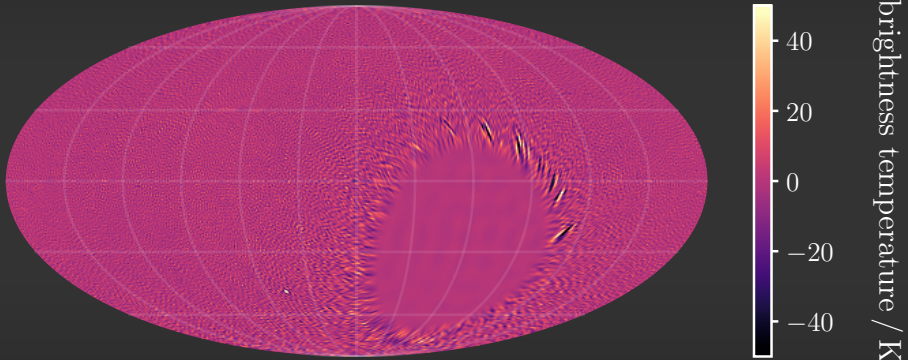
## Comparison with DRAO 22 MHz

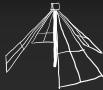


Roger et al. (1999)



## Even–Odd Jackknife

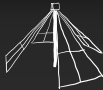




Summary

---

## Day–Night Jackknife



Summary

---

## Filtering Illustration

